Available online at www.sciencedirect.com
ScienceDirect
Scripta Materialia 57 (2007) 1016–1019
Scripta MATERIALIA
www.elsevier.com/locate/scriptamat

# Observation of the failure mechanism for diamond-like carbon film on stainless steel under tensile loading

Hyun-Jong Kim,[a,b] Myoung-Woon Moon,[b] Dong-Ik Kim,[b] Kwang-Ryeol Lee[b] and Kyu Hwan Oh[a,*]

[a] *Department of Materials Science and Engineering, Seoul National University, 56-1, Shilim-Dong, Kwanak Gu, Seoul 151-744, South Korea*
[b] *Korea Institute of Science and Technology, 39-1, Hawolgok-Dong, Seungbuk Gu, Seoul 136-791, South Korea*

Received 29 June 2007; revised 30 July 2007; accepted 31 July 2007
Available online 5 September 2007

This study investigated the fracture behaviour of cohesive cracking and subsequent buckling delamination at the interface between a diamond-like carbon (DLC) film and a stainless steel substrate during tension testing. It was revealed by cross-sectional analysis with a focused ion beam system that spallation of the DLC film was caused by interfacial cracking and the subsequent kinking into a thin film layer. Interfacial adhesion strength was estimated by the spalled crack width, which shows that the adhesion of the DLC coating was considerably improved by increasing the negative bias voltage during Ar plasma etching prior to the film deposition.


*Keywords:* Fracture; Thin film; Tension test; Interface adhesion strength

Metallic materials, such as stainless steels and titanium alloys, have been widely used as implant materials for replacing failed hard tissues in biological applications [1]. However, wear behaviour of the metallic materials limits the lifetime of the implants or medical devices [2]. Inadequate compatibility of the implant surfaces and bone tissues could also result in a longer healing time, fixation failures and undesirable inflammatory responses [3,4]. To overcome these issues in metallic implant materials, researchers have adopted coating materials, such as diamond-like carbon (DLC), which have higher wear resistance, as well as high levels of biocompatibility according to in vitro analysis of their interactions with recognized animal [5] and human cell lines [6]. DLC coatings have been known to extend the operational lives of hip and knee prostheses, implantable joints and medical instrumentation [7–9].

In a biological environment, the cracking and interface delamination of coated materials on metal substrates have been frequently observed when compressive or tensile stress is applied [9–11]. The mechanics of fracture at the interface between two materials with different mechanical properties have been analyzed in detail by Hutchinson and Evans [12–14]. In the case of a brittle film on a ductile substrate, a cracked film can either remain attached to the substrate or become unattached at the interface, depending on the interface adhesion strength and substrate moduli, as shown in Figure 1.

The present study focuses on the failure analysis of DLC films deposited on steel substrates under microtensile loading. The work provides the mechanism of cohesive cracking and spallation in the films by cross-sectional analysis with a dual-beam focused ion beam system (FIB). Furthermore, the interface adhesion energy was evaluated by measuring the dimensions of the spalled regions for various deposition conditions and adopting a simple analytical solution from fracture analysis [15–17].

The DLC films were deposited onto 304 stainless steel substrates by radiofrequency plasma-assisted chemical vapor deposition, using benzene ($C_6H_6$) as the precursor gas. Steel coupons, 160 μm thick, were machined into a dog-bone shape for tensile loading (detailed in Ref. [11]). Steel surfaces were electropolished to remove the oxide layer and contaminants on the steel substrate, then cleaned with methyl alcohol in an ultrasonic bath, followed by blow-drying with nitrogen. Two sets of specimens were prepared by varying the Ar plasma

* Corresponding author. Fax: +82 2 872 8307; e-mail: kyuhwan@snu.ac.kr

1359-6462/$ - see front matter 
doi:10.1016/j.scriptamat.2007.07.042

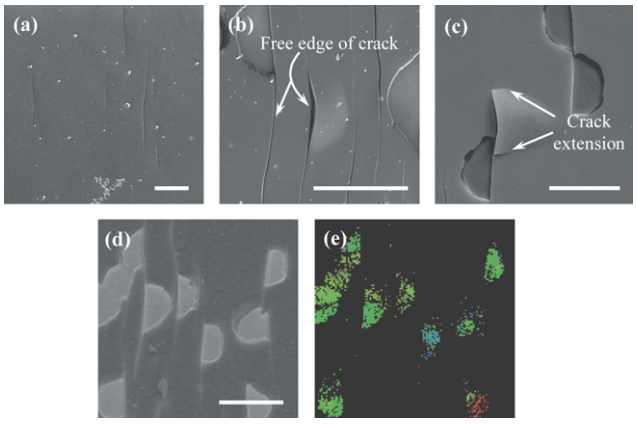


**Figure 1.** SEM images of the DLC films with deposition conditions of Ar plasma etching at −200 V for 30 min and Si buffer layer at −200 V for 5 min. (a) A channel-type cohesive crack occurred at 1.23%; (b) buckling delamination initiated at the free edge of the crack at 1.76%; (c) crack extension at the perimeter of buckling delamination at 2.13%; (d) spallations at 3.55% and (e) EBSD analysis data on the region in (d), with the spalled regions colored green, indicative of the crystalline orientation as a stainless steel material. Bar = 20 μm for the inset. (For interpretation of the references to color in this figure legend, the reader is referred to the web version of this article.)

treatment voltage and buffer layer thickness, respectively. The first set was to observe the etching effect of the Ar plasma on the interface adhesion strength between the DLC films and the steel substrates. The surface of the steel substrate was Ar plasma-etched for 20 min at various self-bias voltages in the range from −200 to −800 V, while the Si buffer layer was deposited for 5 min at a bias voltage of −200 V. The second set was prepared by changing the thickness of the Si buffer layer deposited between the DLC film and the steel substrate. Here Ar plasma treatment was set for 30 min at a bias voltage of −400 V. The Si buffer layer was deposited at a bias voltage −200 V for 2 min 30 s, 5 or 10 min. The DLC film was deposited at a bias voltage −400 V and a working pressure of 1.33 Pa. The thickness and residual stress of the DLC film was 900 ± 10 nm and 0.87–0.9 GPa in compression, respectively.

Using a screw-driven tensile tester [11], the tensile load was applied to the DLC-coated steel substrate under displacement control up to ~20% in strain. Initial film cracking and buckling delamination were carefully observed during the tension test. After the application of each 0.5% strain increment, the specimen's surface was repeatedly observed by a FIB/scanning electron microscopy (SEM) system (Nova 200, FEI). The local strain ($\varepsilon_s$) near the failure site was estimated by the change in the shape of the indented markers that had been fabricated using a diamond-shaped indenter before the DLC coating. The cracks in the film and interface were characterized by the serial sectionings at the failure sites (Figs. 3 and 4).

The cohesive cracks in the film first appeared perpendicular to the axis of tensile loading at a strain of 1.23%. Figure 1a shows the channel-type cohesive cracking. The cohesive crack plays an important role as a flaw initiating the interface delamination [18]. Upon further straining, subsequent buckling delamination occurred at the free edge of the cohesive crack due to the high energy release rate and compressive strain developed by Poisson's contraction normal to the tensile direction, as shown in Figure 1b [15]. DLC film was cracked at the perimeter of the buckling delamination and remained a semi-circular shape (see Fig. 1c and d). The surface material exposed after the spallation of the DLC layer was stainless steel (green color in Fig. 1e), as confirmed by electron backscattered diffraction (EBSD) analysis.

Figure 2 shows the density of cracks in the coating for the bias voltages during the Ar plasma treatment of −200 and −600 V. For the case of the bias voltage of −200 V, the onset strain of the cohesive crack was 1.23% and that for the spallation 1.76%. Increasing the bias voltage to −600 V increased both onset strains. The onset strains for the cohesive cracking and the spallation were 1.65% and 19.17%, respectively. The result shows that the initial onset strain for the cohesive crack of the DLC coating increased slightly as the bias voltage during the Ar plasma treatment increased. However, one should note that the onset strain for the spallation was dramatically increased from 1.76% to 19.17%, indicative of a significant improvement in adhesion strength at the interface [19,20]. The average spacings between the cohesive cracks were, respectively, about 7.5 and 3.5 μm as measured in the SEM images. Previous theoretical analysis showed that the crack spacing would decrease under better adhesion conditions because misfit stress between the film and substrate would transfer into the film without interface failures [21,22]. The change in the spacing of the cohesive crack also confirmed that the adhesion strength increased with the negative bias voltage during the Ar plasma treatment.

The region with cohesive cracks in the films was examined using sectional analysis with FIB (see Fig. 3a). At an initial strain of 1.02%, the crack tip propagated through the thickness of the DLC film and stopped at the interface, as shown in Figure 3b. As the tensile strain increased, the steel substrate plastically deformed and the spacing between the crack edges of the film increased, as shown in Figure 3c. It was also

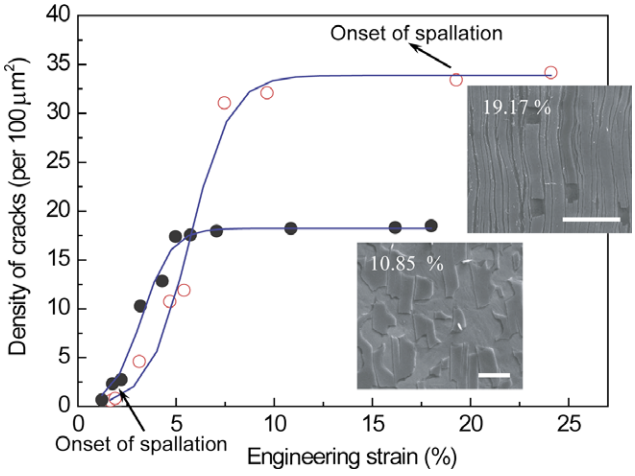


**Figure 2.** A plot of the density of cracks with applied engineering strain under different adhesion conditions. Solid circles and open circles denote two different adhesion conditions with Ar plasma treatment at −200 and −600 V, respectively. Bar = 20 μm.

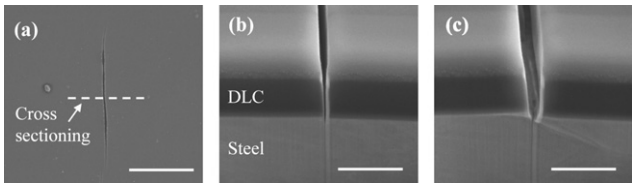


**Figure 3.** (a) A cohesive crack in DLC film; bar = 10 μm. (b) A cross-sectional view of the cohesive crack using FIB sectioning at a tensile strain at 1.02%. (c) After further straining at 4.57%, the distance between the free edges became wider; bar = 1 μm. Deposition conditions of Ar plasma etching at −600 V for 50 min and Si interlayer at −200 V for 10 min.

observed that plastic deformation of the steel substrate tends to blunt the crack tip at the interface, resulting in suppression of the propagation of the cohesive crack into the steel substrate.

For a tensile strain beyond a critical value, interface delamination starts from a free edge of the cohesive crack due to the high energy release rate. As the width of the buckle reaches a critical value, the kink at the crack fronts of the buckle was observed, as shown in Figure 4. When the interface is relatively tough, the trajectory of the interface crack appears to be driven off the interface into the film, which may increase mode I fracture [15,23–25]. The kinked cracks that developed at both edges of the buckle (bottom left and right in Fig. 4) extend along the crack front of the buckling delamination. The kinking of the DLC films eventually causes the spallation on the substrate. Finally, the entire buckled region was spalled off in the shape of a semi-circle, as shown in Figure 1d. The width, $2b$, of the spalled region of the DLC film depends on the pretreatment conditions. The widths are plotted in Figure 5a for various values of the bias voltages during Ar plasma etching and the thickness of the Si buffer layer. As the thickness of the Si buffer layer increased, the spalled width ($2b$) gradually decreased. Increasing the bias voltage during the Ar plasma etching significantly reduces the spalled width when the bias voltage is beyond −600 V. The width of the spalled region was used to

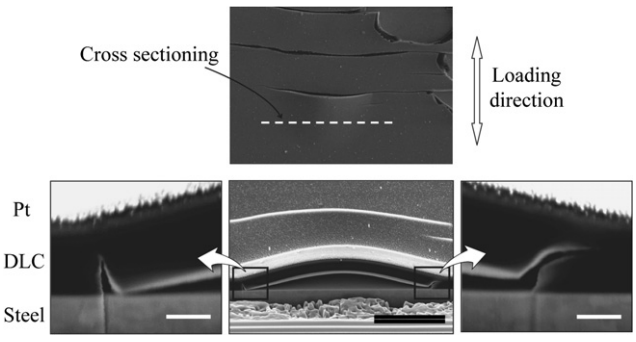


**Figure 4.** A cross-sectional view of the buckling delamination as seen by SEM. Top: buckling delamination initiated at a free edge of a cohesive crack; bottom middle: cross-section of buckling delamination (bar = 5 μm); bottom left and right: magnification of the kinked sites at each edge of the interface crack noted as square boxes (bar = 500 nm) (deposition conditions: Ar plasma etching at −600 V for 50 min and Si buffer layer at −200 V for 10 min). The Pt layer was pre-deposited to prevent $Ga^+$ ion beam damage during FIB sectioning.

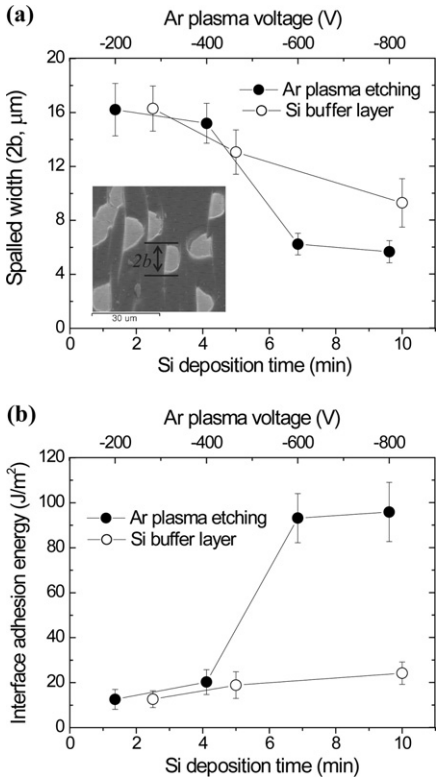


**Figure 5.** (a) A plot for the width ($2b$) of the spalled region with voltage for the Ar plasma treatment (solid circle) and deposition time for the Si buffer layer (open circle). (b) A plot for the interfacial adhesion energy estimated using Eq. (1) and experimental data from (a).

quantitatively evaluate the interface adhesion energy for various conditions using a simple analytical solution, as will be discussed below [15–17].

By a simple assumption of a circular blister model for buckling delamination, the interface adhesion energy was estimated using the buckled width with respect to deposition conditions. Under the condition of the fully steady-state for the crack propagation of a circular buckle, the steady-state energy release rate, $G$, averaged over the strain energy per unit area in the unbuckled film, $G_0 = (1 - \nu_f)h\sigma^2/E_f$, could be expressed as $G/G_0 = c_2[1 - (\sigma_c/\sigma)^2]$, where the classical buckling stress ($\sigma_c$) is $1.2235[E_f/(1 - \nu_f^2)](h/b)^2$. Here $E_f$ and $\nu_f$ are the Young's modulus and the Poisson's ratio in the film, respectively, and $c_2 = [1 + 0.9021(1 - \nu_f)]^{-1}$ [15]. The applied stress ($\sigma$) in the film is determined from a summation of the initial residual stress ($\sigma_{res}$) in the DLC film [11] and the applied Poisson's contraction stress ($\nu_s$ $\sigma_s$) in the steel substrate with the Poisson's ratio $\nu_s$ and applied tensile stress $\sigma_s$. Using the definition of $b_0$ as a critical half width for the onset buckling [15,16] and $b$ as the half width of the spalled region, it is convenient to use the expression $(\sigma_c/\sigma) = (b_0/b)^2$ for the purpose of evaluation of the interface adhesion energy ($\Gamma_c$) as

$$\Gamma_c = G = c_2 G_0 \left[1 - \left(\frac{b_0}{b}\right)^4\right], \quad (1)$$

where the pre-determined values of the thickness, stress, elastic modulus and buckled (or spalled) width could be

taken from experimental results shown in Figure 5a. Using Eq. (1), the range of interface adhesion energy was estimated to be 12–98 J $m^{-2}$ for the experiment set with various bias voltages during the Ar plasma etching, as shown in Figure 5b. The estimated values of interface adhesion energy in this work were larger than those for DLC films with the condition of spontaneous buckling delamination (4–6 J $m^{-2}$) [16,18]. However, the estimated range of the interface adhesion energy is feasible since adhesion strength was significantly improved by the Ar plasma treatment and the Si buffer layer. In the previous works, the poor adhesion condition had been carefully chosen for the purpose of achieving the buckling delamination in the DLC film on a glass substrate [16]. From the result shown in Figure 5b, it was also evident that the increment in the bias voltage of Ar plasma is a more effective way to improve the interface adhesion strength of the DLC coating on steel substrates [19,20].

In summary, fracture behaviours of brittle film on ductile substrate were analyzed with a tension test. During uniaxial tensile loading, the film showed cohesive cracks normal to the tensile loading followed by the buckling delaminations initiated from free edges of the cohesive cracks by Poisson's contraction. The width, 2*b*, of the buckled region extends until it reaches a critical value at which the interface adhesion strength is matched by the kinking strength. Then, the trajectory of an interfacial crack appears to be driven off the interface and kinked into the DLC film, causing the spallation of DLC film in a semi-circular shape. The sizes of the spalled regions were adopted to quantitatively evaluate the interface adhesion energy for each set of deposition conditions using a simple analytical solution. In this study, the interface adhesion energy was increased to the range of 12–98 J $m^{-2}$ by optimizing the condition of the Ar plasma treatment and Si buffer layer deposition.

This research was supported by a Grant (No. 06K1501-01613) from "Center for Nanostructured Materials Technology" under "21st Century Frontier R&D Programs" of the Ministry of Science and Technology, Korea and Taewoong Medical Inc. Ltd. The authors would like to acknowledge fruitful discussions with Prof. John W. Hutchinson, from Harvard University, USA, and Dr. Jae-Hyun Kim, from KIMM, South Korea.

[1] N. Mitsuo, Metall. Mater. Trans. 33A (2002) 477.
[2] R. Hauert, Diamond Relat. Mater. 12 (2003) 583.
[3] Y.C. Tsui, C. Doyle, T.W. Clyne, Biomaterials 19 (1998) 2015.
[4] C.P.A.T. Klein, P. Patsa, J.G.C. Wolke, J.M.A. Blieck-Hogervorst, K. Groot, Biomaterials 15 (1994) 146.
[5] L.A. Thomson, F.C. Law, N. Rushton, J. Franks, Biomaterials 12 (3) (1991) 37.
[6] M. Allen, F. Law, N. Rushton, Clin. Mater. 17 (1994) 1.
[7] S. Aisenberg, J. Vac. Sci. Tcchnol. A 2 (1984) 369.
[8] J. Franks, J. Vac. Sci. Technol. A 7 (1989) 2307.
[9] A.A. Ogwu, T. Coyle, T.I.T. Okpalugo, P. Kearney, P.D. Maguire, J.A.D. McLaughlin, Acta Mater. 51 (2003) 3455.
[10] P.D. Maguire, J.A.D. McLaughlin, T.I.T. Okpalugo, P. Lemoine, P. Papakonstantinou, E.T. McAdams, M. Needham, A.A. Ogwu, M. Ball, G.A. Abbas, Diamond Relat. Mater. 14 (2005) 1277.
[11] H.W. Choi, K.R. Lee, R. Wang, K.H. Oh, Diamond Relat. Mater. 15 (2006) 38.
[12] M.S. Hu, A.G. Evans, Acta Metal. 37 (1989) 917.
[13] A.G. Evans, M.D. Drory, M.S. Hu, J. Mater. Res. 3 (1988) 1043.
[14] M.Y. He, A.G. Evans, J.W. Hutchinson, Mater. Sci. Eng. A 245 (1998) 168.
[15] J.W. Hutchinson, Z. Suo, Adv. Appl. Mech. 29 (1992) 63.
[16] M.W. Moon, H.M. Jensen, J.W. Hutchinson, K.H. Oh, A.G. Evans, J. Mech. Phys. Solids 50 (2002) 709.
[17] A. Lee, B.M. Clemans, W.D. Nix, Acta Mater. 52 (2004) 2081.
[18] M.W. Moon, J.W. Chung, K.R. Lee, K.H. Oh, R. Wang, A.G. Evans, Acta Mater. 50 (2002) 1219.
[19] B.A. Latella, G. Triani, Z. Zhang, K.T. Short, J.R. Bartlett, M. Ignat, Thin Solid Films 515 (2007) 3138.
[20] M. Joinet, O. Borrod, L. Thomas, C. Picard, V. Lucas, F. Teyssandier, Diamond Relat. Mater. 16 (2007) 1254.
[21] B.A. Latella, G. Triani, P.J. Evans, Scripta Mater. 56 (2007) 493.
[22] J.H. Jeong, D.I. Kwon, J. Adhes. Sci. Technol. 12 (1) (1998) 29.
[23] M.Y. He, A. Bartlett, A.G. Evans, J. Am. Ceram. Soc. 74 (4) (1991) 767.
[24] M.D. Thouless, H.C. Cao, P.A. Mataga, J. Mater. Sci. 24 (1989) 406.
[25] M.Y. He, J.W. Hutchinson, Int. J. Solids Struct. 25 (9) (1989) 1053.